Anisotropic Propagating Excitations and Quadrupolar Effects in $Tb_2Ti_2O_7$

Solène Guitteny,[1] Julien Robert,[1] Pierre Bonville,[2] Jacques Ollivier,[4] Claudia Decorse,[3] Paul Steffens,[4] Martin Boehm,[4] Hannu Mutka,[4] Isabelle Mirebeau,[1] and Sylvain Petit[1]

[1]*Laboratoire Léon Brillouin, CEA Saclay, Bâtiment 563, 91191 Gif-sur-Yvette Cedex, France*
[2]*DSM/IRAMIS/SPEC, CEA Saclay, 91191 Gif-sur-Yvette Cedex, France*
[3]*ICMMO, Université Paris 11, 91405 Orsay, France*
[4]*Institut Laue Langevin, 6 rue Jules Horowitz, Boîte Postale 156, F-38042 Grenoble, France*

(Received 2 May 2013; revised manuscript received 5 July 2013; published 20 August 2013)

The dynamical magnetic correlations in $Tb_2Ti_2O_7$ have been investigated using polarized inelastic neutron scattering. Dispersive excitations are observed, emerging from pinch points in reciprocal space and characterized by an anisotropic spectral weight. Anomalies in the crystal field and phonon excitation spectrum at Brillouin zone centers are also reported. These findings suggest that Coulomb phases, although they present a disordered ground state with dipolar correlations, allow the propagation of collective excitations. They also point out a strong spin-lattice coupling, which likely drives effective interactions between the $4f$ quadrupolar moments.

DOI: 10.1103/PhysRevLett.111.087201 PACS numbers: 75.50.Ee, 75.10.Jm

In the last decade, spin-ice physics in the $R_2Ti_2O_7$ rare-earth pyrochlore, the celebrated lattice of corner sharing tetrahedra considered as the archetype of geometrical frustration in three dimensions, has aroused a lot of attention [1,2]. At the heart of this interest is a local constraint stating that each tetrahedron of the pyrochlore lattice must have, in its ground state, two spins pointing in and two spins pointing out, the so-called "two-in–two-out" ice rule, leading to a macroscopic degeneracy and to an emergent gauge structure [3,4]. The classical spins are quenched into one of the degenerate ground states formed by these configurations, resulting in an analog of water ice [5,6]. One of the main characteristics of this "Coulomb phase" is the existence of power law dipolar spin correlations, resulting in distinctive sharp and anisotropic features, the so-called "pinch points," in neutron diffraction patterns [4].

Other nontrivial states of matter may be produced in the quantum variant of spin ices. In this case, appreciable fluctuations between degenerate configurations are restored, resulting in a spin liquid state [7–9]. Current theoretical descriptions introduce a minimal pseudospin-1/2 Hamiltonian, spanning the crystal electric field (CEF) ground doublet states $|\pm\rangle$, together with an Ising exchange constant J_{zz} responsible for the spin-ice behavior, as well as "quantum" transverse terms $J_{\pm}$, $J_{z\pm}$, and $J_{\pm\pm}$ [7,10]. For such large transverse terms, conventional phases are stabilized. They are characterized by a classical dipolar ordering in the case of Kramers ions and by a quadrupolar ordering of the $4f$ quadrupoles for non-Kramers ions [9–11], accompanied by a coupling to the lattice degrees of freedom. The quantum spin-ice behavior is expected for moderate couplings, and the ground state is a Coulomb phase described by an intricate superposition of two-in–two-out configurations [7,8]. It exhibits exotic excitations with especially a two spinon continuum, as well as an emergent photon associated with the gauge structure [12].

A potential candidate for this particular regime is $Tb_2Ti_2O_7$. It is characterized by an Ising-like anisotropy of the non-Kramers Tb^{3+} ions along the local $\langle 111\rangle$ axes [8,13]. In spite of effective antiferromagnetic interactions leading to a Curie-Weiss temperature of -13 K [14], which should drive the system into long-range order [15,16], prior works pointed out a disordered fluctuating ground state down to 20 mK [17,18]. Various subsequent studies have suggested complex spin dynamics, where different time and temperature scales coexist, as revealed by muons [19–21], magnetization [22,23], and neutron scattering experiments [24–33]. Recently, power law spin correlations have also been reported [34], bearing some resemblance to the pinch-point pattern observed in the aforementioned dipolar spin ices [35] and suggesting that the ground state of this material might be a Coulomb phase.

To go further, we report in this Letter a detailed description of the excitations emanating from this particular ground state. Combined elastic and inelastic neutron scattering measurements with polarization analysis provide evidence for the existence of low energy propagating excitations. Anomalies of the phonon modes, as well as of the first CEF level, are also observed, which unveil a strong dynamical coupling with the lattice.

Low energy neutron experiments ($\hbar\omega \lesssim 0.5$ meV) were carried out on the 4F2 and IN14 triple axis spectrometers installed at LLB-Orphee (Saclay, France) and at the Institute Laue Langevin (Grenoble, France), respectively. The final energy was fixed to 3 meV, yielding an energy resolution $\Delta_0 \simeq 0.07$ meV (FWHM). Time-of-flight data were also collected on IN5 (ILL), with its recent single crystal setup, with an incident wavelength $\lambda = 4$ Å.

The magnetic correlations of several pyrochlore magnets have been studied in detail by means of neutron diffraction [34]. Indeed, this technique provides a direct

measurement of the spin pair correlation function $M(\mathbf{Q}) = \sum_{i,j}\langle \mathbf{S}_{\perp,i}\mathbf{S}_{\perp,j}\rangle e^{-i\mathbf{Q}\cdot\mathbf{r}_{ij}}$, where $\mathbf{S}_{\perp,i}$ denotes the spin component at site i perpendicular to the wave vector $\mathbf{Q}$. In dipolar spin ices, in which the spins are confined along the local easy axes $\langle 111\rangle$, it has been possible to measure the usual two-in–two-out correlations [34] by performing polarized neutron scattering experiments in the (h, h, l) scattering plane, experiments which are sensitive to the directions of the spin-spin correlations. Those correlations are observed in the so-called "M_y" channel [35]. In $Tb_2Ti_2O_7$, the weaker anisotropy allows the spins to move away from their easy axes, resulting in additional correlations between the transverse spin components perpendicular to $\langle 111\rangle$. The so-called "M_z" channel allows us to measure those correlations (restricted, however, to spin components along the z vertical axis $\parallel [1\bar{1}0]$) and points out antiferromagnetic "two-up–two-down" spin configurations [35]. Both kinds of correlations present pinch points at the Brillouin zone centers but show maxima at different places in $\mathbf{Q}$ space [34]. For instance, the vicinity of $\mathbf{Q} = (2, 2, 0)$ is dominated by two-up–two-down' transverse correlations (strong M_z) while $\mathbf{Q} = (1, 1, 1)$ is dominated by two-in–two-out–like correlations (strong M_y).

Diffraction provides, however, an energy-integrated response, so that energy resolved experiments, measuring $M(\mathbf{Q}, \omega) = \int dt \sum_{i,j}\langle \mathbf{S}_{\perp,i}\mathbf{S}_{\perp,j}(t)\rangle e^{i(\omega t - \mathbf{Q}\cdot\mathbf{r}_{ij})}$ are important to further characterize the correlations. In this context, elastic $\omega = 0$ data, obtained at $T = 0.05$ K, are shown in Fig. 1(a). They are in qualitative agreement with the polarized data reported in Ref. [35]. No magnetic Bragg peaks could be detected at $(1/2, 1/2, 1/2)$, as reported in $Tb_{2+x}Ti_{2-2x}Nb_xO_7$ [36] and $Tb_{2+x}Ti_{2-x}O_{7+y}$ [29]. This is consistent with the lattice parameter [$a = 10.1528(5)$ Å], determined precisely using x-ray scattering, and which

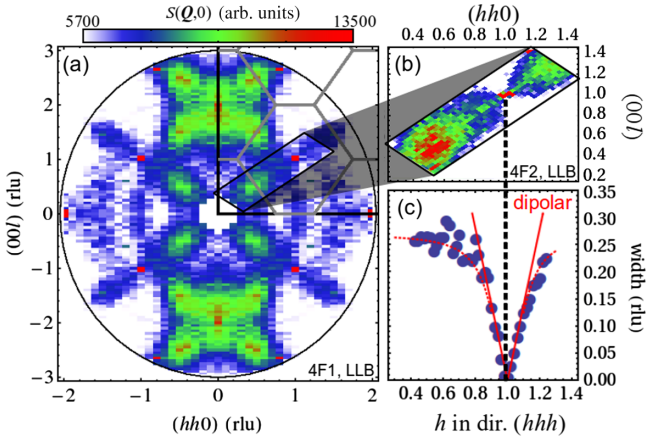

FIG. 1 (color online). (a) Map of the $\omega = 0$ (elastic) scattering at $T = 0.05$ K. The data within the top left corner have been actually measured and then symmetrized. Gray lines correspond to the boundaries of Brillouin zones. The data in (b) have been measured with smaller $\mathbf{Q}$ steps, focusing on the region close to the (111) pinch point. (c) A fit of the width along $q_\perp$ for different $q_\parallel$ varying along $\langle h, h, h\rangle$, as described in the text.

positions our $Tb_2Ti_2O_7$ sample in the spin liquid phase [29]. Focusing on the vicinity of $\mathbf{Q} = (2, 2, 0)$, a two-up–two-down static correlation length of about $\xi = 5 \pm 1$ Å was determined by fitting the width of the corresponding pinch point in the l direction (not shown). This value is comparable with the (energy-integrated) diffraction results $\xi = 2 \pm 0.2$ Å. A similar analysis around $\mathbf{Q} = (1, 1, 1)$ points out longer-range two-in–two-out correlations, as seen in Fig. 1(b). Following Ref. [4], the structure factor close to the pinch point was fitted through a Lorentzian profile $q_\parallel^2/(q_\perp^2 + q_\parallel^2 + 1/\xi^2)$, with $q_\parallel$ along $\langle h, h, h\rangle$, $q_\perp$ in the transverse direction, and ξ the static correlation length. An excellent agreement is obtained, as shown in Fig. 1(c). The experimental width at the pinch point is limited by the instrument resolution, leading to $\xi > 80$ Å, at least 1 order of magnitude larger than the instantaneous one obtained from diffraction results ($\xi = 8 \pm 2$ Å). These energy resolved data thus show that integrating over energy actually blurs very well-defined pinch points, thus pointing out sizable magnetic fluctuations.

To further characterize the spectrum of these low energy fluctuations [24–33], polarized neutron experiments have been carried out on IN14, using the $M_{y,z}$ decomposition described above. Figure 2 shows raw data taken at constant $\mathbf{Q} = (220)$ [Fig. 2(a)], as well as M_y and M_z [37] for different scattering vectors along high symmetry directions $\langle h, h, 2-h\rangle$ [Figs. 2(b)–2(d)] and $\langle h, h, h\rangle$ [Figs. 2(e)–2(g)]. These measurements show the existence of a dual response consisting of both an inelastic (blues squares) and a quasielastic (red disks) signal, as pointed out in Ref. [28]. The M_z contribution is always found to be quasielastic. This is consistent with the very short-range character of the two-up–two-down correlations, which may eliminate any possibility for coherent excitations to propagate.

In contrast, M_y is different, whether $\langle h, h, h\rangle$, $\langle h, h, 2-h\rangle$, or $\langle h, h, 0\rangle$ is considered. Along $\langle h, h, h\rangle$, it is dominated by a quasielastic signal comparable to M_z [Figs. 2(e)–2(g)]. Its intrinsic width (FWHM), roughly $\mathbf{Q}$ independent, is around $\Gamma \simeq 0.15$ meV, providing a relaxation time $\tau \simeq 1.5$ ps at $T = 0.05$ K. Along $\langle h, h, 2-h\rangle$ and $\langle h, h, 0\rangle$, M_y shows gapless propagating excitations. The data have been fitted using a Lorentzian profile multiplied by the Bose factor and convoluted with the experimental resolution function. This provides the width, intensity, and energy position of the mode reported in Figs. 3(b) and 3(c). Stemming from the pinch point at (1,1,1), it disperses significantly up to $\simeq 0.3$ meV at (2,2,0), albeit more weakly along $\langle h, h, 0\rangle$. The presence of a small gap cannot be completely ruled out (at an energy, however, smaller than the experimental resolution $\Delta_0 = 0.07$ meV). Furthermore, as shown in Fig. 3(b), the intensity of the mode along $\langle h, h, 2-h\rangle$ decreases as $1/\omega$, a usual feature of magnetic excitations. This is very different from the behavior expected for the emergent photon, recently put forward in Ref. [12], and whose intensity is expected to grow as $\propto \omega$. A significant decrease of the spectral weight

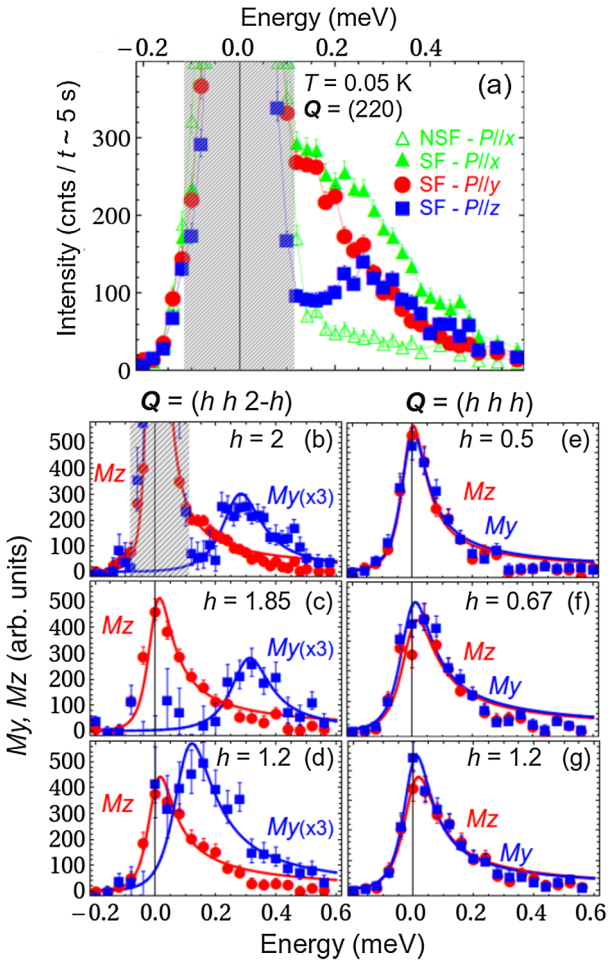

FIG. 2 (color online). (a) Spin-flip (SF) (polarization $\mathbf{P}\|\mathbf{x},\mathbf{y},\mathbf{z}$) and non-spin-flip (NSF) ($\mathbf{P}\|\mathbf{x}$) raw scans for $Q=(220)$ and $T=0.05$ K. The $\mathbf{x}$ ($\|\mathbf{Q}$) and $\mathbf{y}$ ($\perp\mathbf{Q}$) in the scattering plane and $\mathbf{z}$ ($\|[1\bar{1}0]$) axes are defined according to the spectrometer frame. (b)–(d) [respectively, (e)–(g)] show M_y and M_z obtained by combining the different raw data [37] with a flipping ratio FR $\simeq$ 20 in direction $\langle h, h, 2-h\rangle$ (respectively, $\langle h, h, h\rangle$). The hatched areas hide the regions where the polarization analysis fails to suppress the nuclear background (Bragg peak contribution). The lines are the result of a fit (as described in the text).

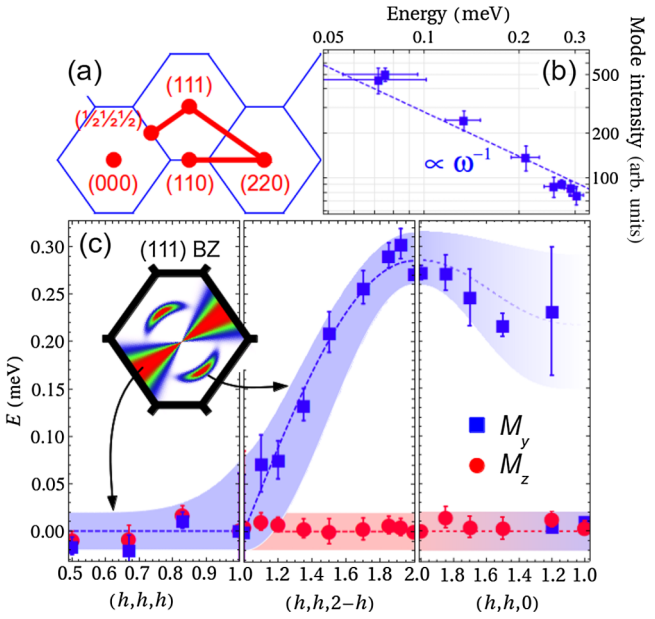

FIG. 3 (color online). (a) Sketch of the Brillouin zone indicating the directions of the scans carried out in the present study. (b) The evolution of the intensity of the dispersive inelastic mode as a function of ω along $\langle h, h, 2-h\rangle$. (c) The dispersion of the mode along the three high symmetry directions. The inset is a schematic map of the M_y spectral weight distribution in the Brillouin zone, which superimposes both the quasistatic (along $\langle h, h, h\rangle$) and the inelastic ("half moon") contributions.

is also observed close to (1,1,0). The propagation of such a collective excitation may be due to the spatial stiffness associated with the presence of algebraic correlations. The intrinsic width of the mode is, however, slightly larger than the resolution, a damping effect specific to systems having a strongly fluctuating ground state [38,39].

To illustrate M_y's peculiar spectral weight distribution, the inset of Fig. 3 illustrates a constant energy cut taken in the vicinity of the pinch point at (1,1,1). The feature along (1,1,1) corresponds to quasistatic spin-ice-like correlations, while propagating excitations are visible along $\langle h, h, 2-h\rangle$ and form the "half moon" features. This peculiar spectral weight distribution in reciprocal space can be understood by considering that the mode propagates defects which break the local constraint, hence giving rise to some response at positions in $\mathbf{Q}$ space which are in principle forbidden by the ice rule. Such observations have already been made numerically in the classical antiferromagnetic Heisenberg model on the pyrochlore [40,41], kagome [38], and checkerboard [41] lattices, all of those systems exhibiting local constraints and pinch-point singularities. From these considerations, it follows that this anisotropic spectral weight could be an intrinsic feature of Coulomb phases, a hypothesis that will have to be confirmed in further theoretical studies.

At slightly larger energies $\hbar\omega \sim 1$–2 meV, the inelastic response is dominated by the first CEF excitations [42] located at $\Delta \approx 1.5$ meV. Since Δ is small, especially compared to classical spin ices (where $\Delta \sim 20$ to 30 meV), the first CEF level is expected to play a significant role in the low energy properties of the system [14,16,25]. The line shape of this CEF excitation is much more complicated than a single dispersionless mode and very likely contains two different modes (not shown). It is strongly modulated at 10 K and down to the base temperature of 50 mK because of the interactions between Tb^{3+} magnetic moments [16]. In a very narrow range of scattering vectors $\mathbf{Q}$ close to crystalline zone centers, such as (1,1,1) and (2,2,0), an unexpected upturn of the dispersion is observed [see Fig. 4(a)]. This upturn arises within the region of reciprocal space where there is a crossing between the crystal field level and the acoustic phonon branch stemming from the zone centers. Here, the phonon and the CEF seem to repel each other. To further illustrate this point, different cuts along $\langle h, h, h\rangle$ have been taken at different energy transfers from 0 to 3 meV. Figure 4(b) shows

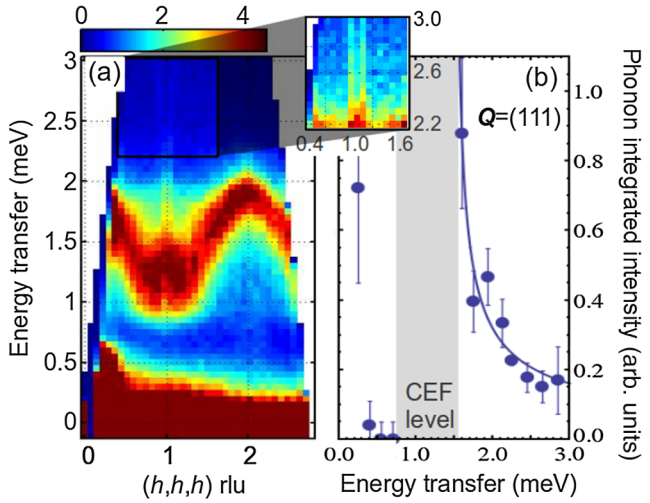

FIG. 4 (color online). (a) IN5 data showing the inelastic scattering as a function of energy transfer ω and Q along $\langle h, h, h\rangle$. The data have been taken at 1.5 K, but similar results are observable at 10 K. The crossing of the acoustic phonon mode and the dispersing CEF occurs close to $Q = (1, 1, 1)$. The inset has been plotted using a different intensity scale (from 0 to 1) to highlight the two branches of the acoustic phonon dispersion. (b) Simultaneously, the intensity of the phonon as a function of energy is strongly suppressed below the CEF line and recovers an usual behavior above.

the corresponding $\mathbf{Q}$-integrated intensity of the phonon plotted as a function of ω. In classical cases, it simply scales as $1/\omega$; in the present case, however, a suppression of the phonon intensity below the CEF is observed. These features are the sign of a strong magnetoelastic coupling, although, here, the CEF level and the acoustic phonon do not seem to follow conventional hybridization processes [43–45].

The issue remains to relate the low energy propagating excitations and the strong magnetoelastic coupling. The existence of the former is indeed an intriguing question: because of the intrinsic properties of non-Kramers magnetic doublets, there are no matrix elements between the time conjugate states of the doublet $|\pm\rangle$ [46], leading to a neutron cross section $|\langle +|\hat{\mathbf{J}}|-\rangle|^2 = 0$. Nonzero matrix elements might in principle be restored by including the first excited CEF level [8,47]. However, as long as the exchange terms are 1 order of magnitude weaker than Δ, the perturbed wave function should not depart too much from $|\pm\rangle$, thus resulting in a vanishingly small inelastic spectral weight [48,49].

To recover a significant cross section, it is therefore essential to go beyond a dipolar Hamiltonian and to consider, for example, a coupling between quadrupolar moments [28,47]. In this respect, the magnetoelastic coupling responsible for the phonon and the CEF anomalies (see Fig. 4) could be the driving force leading to effective interactions between quadrupoles [43]. There are additional clues in favor of a strong dynamical spin-lattice coupling: structural fluctuations below 15 K observed by high resolution X diffraction [50], giant magnetostriction [51], and the instability of the spin liquid state versus pressure and stress [52], all of which have been reported recently, but no static distortion has been observed so far [53].

A model based on the most simple on-site quadrupolar term has been proposed, phenomenologically connected with a possible tetragonal distortion precursor to a $T \simeq 0$ Jahn-Teller transition [20,28,47–49,54–56]. Despite being rather successful in explaining a number of experimental results [28,49,57], it does not, in its present form, capture the whole nature of the ground state; for instance, it leads to a CEF singlet state on each site, which is not compatible with the existence of static correlations (see Fig. 1). Finding a more appropriate set of quadrupolar terms might be achieved on the basis of recent effective pseudospin-1/2 models [9,11]. However, since the low energy branch is not the predicted emergent photon [12], the suitability of this approach to model $Tb_2Ti_2O_7$ remains unclear. Models based on several gauge fields [58] to account for the role of transverse spin components could be better suited, but the coupling between the $4f$ quadrupolar moments should definitely be considered.

In summary, our neutron results demonstrate the existence of a low energy propagating excitation emanating from the spin liquid ground state of $Tb_2Ti_2O_7$. Its peculiar spectral weight distribution could be the signature of propagating defects, breaking the divergence-free flux characteristic of the Coulomb phase. We also report anomalies of the phonon modes, as well as of the first CEF level, suggesting a strong dynamical coupling to the lattice. These experimental findings emphasize the importance of quadrupolar interactions in the physics of non-Kramers ion-based quantum spin ices.

The authors acknowledge fruitful discussions with M. Gingras, B. Canals, E. Lhotel, and A. Goukassov. We also acknowledge F. Damay for a careful reading of the manuscript.

[1] C. Lhuillier and G. Misguich, in *Introduction to Frustrated Magnetism*, edited by C. Lacroix, Ph. Mendels, and F. Mila (Springer, New York, 2011).
[2] J. S. Gardner, M. J. P. Gingras, and J. E. Greedan, Rev. Mod. Phys. **82**, 53 (2010).
[3] S. V. Isakov, K. Gregor, R. Moessner, and S. L. Sondhi, Phys. Rev. Lett. **93**, 167204 (2004).
[4] C. L. Henley, Phys. Rev. B **71**, 014424 (2005).
[5] S. T. Bramwell, M. J. Harris, B. C. den Hertog, M. J. P. Gingras, J. S. Gardner, D. F. McMorrow, A. R. Wildes, A. L. Cornelius, J. D. M. Champion, R. G. Melko, and T. Fennell, Phys. Rev. Lett. **87**, 047205 (2001); S. T. Bramwell and M. J. P. Gingras, Science **294**, 1495 (2001).
[6] C. Castelnovo, R. Moessner, and S. L. Sondhi, Phys. Rev. Lett. **104**, 107201 (2010).
[7] M. Hermele, M. P. A. Fisher, and L. Balents, Phys. Rev. B **69**, 064404 (2004).
[8] H. R. Molavian, M. J. P. Gingras, and B. Canals, Phys. Rev. Lett. **98**, 157204 (2007).
[9] S. Onoda and Y. Tanaka, Phys. Rev. Lett. **105**, 047201 (2010); S. Onoda and Y. Tanaka, Phys. Rev. B **83**, 094411 (2011).
[10] L. Savary and L. Balents, Phys. Rev. Lett. **108**, 037202 (2012).

[11] S. B. Lee, S. Onoda, and L. Balents, Phys. Rev. B **86**, 104412 (2012).

[12] O. Benton, O. Sikora, and N. Shannon, Phys. Rev. B **86**, 075154 (2012).

[13] H. Cao, A. Gukasov, I. Mirebeau, P. Bonville, C. Decorse, and G. Dhalenne, Phys. Rev. Lett. **103**, 056402 (2009).

[14] M. J. P. Gingras, B. C. den Hertog, M. Faucher, J. S. Gardner, S. R. Dunsiger, L. J. Chang, B. D. Gaulin, N. P. Raju, and J. E. Greedan, Phys. Rev. B **62**, 6496 (2000).

[15] B. C. den Hertog and M. J. P. Gingras, Phys. Rev. Lett. **84**, 3430 (2000).

[16] Y.-J. Kao, M. Enjalran, A. Del Maestro, H. R. Molavian, and M. J. P. Gingras, Phys. Rev. B **68**, 172407 (2003).

[17] J. S. Gardner, S. R. Dunsiger, B. D. Gaulin, M. J. P. Gingras, J. E. Greedan, R. F. Kiefl, M. D. Lumsden, W. A. MacFarlane, N. P. Raju, J. E. Sonier, I. Swainson, and Z. Tun, Phys. Rev. Lett. **82**, 1012 (1999).

[18] J. S. Gardner, B. D. Gaulin, A. J. Berlinsky, P. Waldron, S. R. Dunsiger, N. P. Raju, and J. E. Greedan, Phys. Rev. B **64**, 224416 (2001).

[19] J. S. Gardner *et al.*, Phys. Rev. B **68**, 180401(R) (2003).

[20] Y. Chapuis, A. Yaouanc, P. Dalmas de Réotier, C. Marin, S. Vanishri, S. H. Curnoe, C. Vaju, and A. Forget, Phys. Rev. B **82**, 100402(R) (2010).

[21] A. Yaouanc, P. Dalmas de Réotier, Y. Chapuis, C. Marin, S. Vanishri, D. Aoki, B. Fak, L.-P. Regnault, C. Buisson, A. Amato, C. Baines, and A. D. Hillier, Phys. Rev. B **84**, 184403 (2011).

[22] E. Lhotel, C. Paulsen, P. D. de Réotier, A. Yaouanc, C. Marin, and S. Vanishri, Phys. Rev. B **86**, 020410(R) (2012).

[23] S. Legl, C. Krey, S. R. Dunsiger, H. A. Dabkowska, J. A. Rodriguez, G. M. Luke, and C. Pfleiderer, Phys. Rev. Lett. **109**, 047201 (2012).

[24] Y. Yasui, M. Kanada, M. Ito, H. Harashina, M. Sato, H. Okumura, K. Kakurai, and H. Kadowaki, J. Phys. Soc. Jpn. **71**, 599 (2002).

[25] I. Mirebeau, P. Bonville, and M. Hennion, Phys. Rev. B **76**, 184436 (2007).

[26] K. C. Rule, G. Ehlers, J. R. Stewart, A. L. Cornelius, P. P. Deen, Y. Qiu, C. R. Wiebe, J. A. Janik, H. D. Zhou, D. Antonio, B. W. Woytko, J. P. Ruff, H. A. Dabkowska, B. D. Gaulin, and J. S. Gardner, Phys. Rev. B **76**, 212405 (2007).

[27] K. C. Rule, G. Ehlers, J. S. Gardner, Y. Qiu, E. Moskvin, K. Kiefer, and S. Gerischer, J. Phys. Condens. Matter **21**, 486005 (2009).

[28] S. Petit, P. Bonville, I. Mirebeau, H. Mutka, and J. Robert, Phys. Rev. B **85**, 054428 (2012).

[29] T. Taniguchi, H. Kadowaki, H. Takatsu, B. Fak, J. Ollivier, T. Yamazaki, T. J. Sato, H. Yoshizawa, Y. Shimura, T. Sakakibara, T. Hong, K. Goto, L. R. Yaraskavitch, and J. B. Kycia, Phys. Rev. B **87**, 060408R (2013).

[30] B. D. Gaulin, J. S. Gardner, P. A. McClarty, and M. J. P. Gingras, Phys. Rev. B **84**, 140402 (2011).

[31] H. Takatsu, H. Kadowaki, T. J. Sato, J. W. Lynn, Y. Tabata, T. Yamazaki, and K. Matsuhira, J. Phys. Condens. Matter **24**, 052201 (2012).

[32] L. Yin, J. S. Xia, Y. Takano, N. S. Sullivan, Q. J. Li, and X. F. Sun, Phys. Rev. Lett. **110**, 137201 (2013).

[33] K. Fritsch, K. A. Ross, Y. Qiu, J. R. D. Copley, T. Guidi, R. I. Bewley, H. A. Dabkowska, and B. D. Gaulin, Phys. Rev. B **87**, 094410 (2013).

[34] T. Fennell, P. P. Deen, A. R. Wildes, K. Schmalzl, D. Prabhakaran, A. T. Boothroyd, R. J. Aldus, D. F. McMorrow, and S. T. Bramwell, Science **326**, 415 (2009).

[35] T. Fennell, M. Kenzelmann, B. Roessli, M. K. Haas, and R. J. Cava, Phys. Rev. Lett. **109**, 017201 (2012).

[36] B. G. Ueland, J. S. Gardner, A. J. Williams, M. L. Dahlberg, J. G. Kim, Y. Qiu, J. R. D. Copley, P. Schiffer, and R. J. Cava, Phys. Rev. B **81**, 060408 (2010).

[37] Considering a local (x, y, z) frame with $x \parallel Q$ and z vertical, M_y and M_z describe spin components perpendicular to Q but, respectively, within the scattering plane (along the y axis) and perpendicular to the scattering plane along the z axis. M_y (respectively, M_z) is measured in a spin-flip experiment with the spin polarization along z (y); L. P. Régnault, in *Inelastic Neutron Polarization Analysis, Neutron Scattering from Magnetic Material*, edited by T. Chatterji (Elsevier, New York, 2006).

[38] J. Robert, B. Canals, V. Simonet, and R. Ballou, Phys. Rev. Lett. **101**, 117207 (2008).

[39] R. Moessner and J. T. Chalker, Phys. Rev. B **58**, 12 049 (1998).

[40] P. H. Conlon and J. T. Chalker, Phys. Rev. Lett. **102**, 237206 (2009).

[41] M. Taillefumier, J. Robert, and B. Canals (unpublished).

[42] Because of the nominal trigonal symmetry at the rare-earth site, the ground and first excited CEF states of the Tb^{3+} ion are two doublets [14,16,25].

[43] G. A. Gehring and K. A. Gehring, Rep. Prog. Phys. **38**, 1 (1975).

[44] R. J. Birgeneau, J. K. Kjems, G. Shirane, and L. G. Van Uitert, Phys. Rev. B **10**, 2512 (1974).

[45] P. Thalmeier and P. Fulde, Phys. Rev. Lett. **49**, 1588 (1982).

[46] K. A. Mueller, Phys. Rev. **171**, 350 (1968).

[47] S. H. Curnoe, Phys. Rev. B **78**, 094418 (2008).

[48] P. Bonville, I. Mirebeau, A. Gukasov, S. Petit, and J. Robert, Phys. Rev. B **84**, 184409 (2011).

[49] S. Petit, P. Bonville, I. Mirebeau, H. Mutka, and J. Robert, Phys. Rev. B **85**, 054428 (2012).

[50] J. P. C. Ruff, B. D. Gaulin, J. P. Castellan, K. C. Rule, J. P. Clancy, J. Rodriguez, and H. A. Dabkowska, Phys. Rev. Lett. **99**, 237202 (2007).

[51] J. P. C. Ruff, Z. Islam, J. P. Clancy, K. A. Ross, H. Nojiri, Y. H. Matsuda, H. A. Dabkowska, A. D. Dabkowski, and B. D. Gaulin, Phys. Rev. Lett. **105**, 077203 (2010).

[52] I. Mirebeau, I. N. Goncharenko, P. Cadavez-Peres, S. T. Bramwell, M. J. P. Gingras, and J. S. Gardner, Nature (London) **420**, 54 (2002); I. Mirebeau, I. N. Goncharenko, G. Dhalenne, and A. Revcolevschi, Phys. Rev. Lett. **93**, 187204 (2004).

[53] K. Goto, H. Takatsu, T. Taniguchi, and H. Kadowaki, J. Phys. Soc. Jpn. **81**, 015001 (2012).

[54] L. G. Mamsurova, K. S. Pigal'skii, and K. K. Pukhov, JETP Lett. **43**, 755 (1986).

[55] K. C. Rule and P. Bonville, J. Phys. Conf. Ser. **145**, 012027 (2009).

[56] P. Bonville, I. Mirebeau, A. Gukasov, S. Petit, and J. Robert, J. Phys. Conf. Ser. **320**, 012006 (2011).

[57] P. Bonville, S. Petit, I. Mirebeau, J. Robert, E. Lhotel, and C. Paulsen, J. Phys. Condens. Matter **25**, 275601 (2013).

[58] V. Khemani, R. Moessner, S. A. Parameswaran, and S. L. Sondhi, Phys. Rev. B **86**, 054411 (2012).